

Article

A Multiscale Statistical Analysis of Rough Surfaces and Applications to Tribology

Feodor M. Borodich ^{1,*}, Andrey Pepelyshev ^{2,†}  and Xiaoqing Jin ^{1,†}¹ College of Aerospace Engineering, Chongqing University, Chongqing 400044, China; jinxq@cqu.edu.cn² School of Mathematics, Cardiff University, Senghennydd Road, Cardiff CF24 4AG, UK; pepelyshevan@cardiff.ac.uk

* Correspondence: borodichfm@cqu.edu.cn

† These authors contributed equally to this work.

Abstract: Mathematical modelling of surface roughness is of significant interest for a variety of modern applications, including, but not limited to, tribology and optics. The most popular approaches to modelling rough surfaces are reviewed and critically examined. By providing counterexamples, it is shown that approaches based solely on the use of the fractal geometry or power spectral density have many drawbacks. It is recommended to avoid these approaches. It is argued that the surfaces that cannot be distinguished from the original rough surfaces can be synthesised by employing the concept of the representative elementary pattern of roughness (REPR), i.e., the smallest interval (or area) of a rough surface that statistically represents the whole surface. The REPR may be extracted from surface measurement data by the use of the “moving window” technique in combination with the Kolmogorov–Smirnov statistic.

Keywords: roughness; statistics; fractal; multiscale; surface; tribology; friction; multilevel

MSC: 74A55; 62G05; 28A80



Citation: Borodich, F.M.; Pepelyshev, A.; Jin, X. A Multiscale Statistical Analysis of Rough Surfaces and Applications to Tribology. *Mathematics* **2024**, *12*, 1804. <https://doi.org/10.3390/math12121804>

Academic Editors: Julius Kaplunov and Igor Andrianov

Received: 13 May 2024

Revised: 3 June 2024

Accepted: 6 June 2024

Published: 10 June 2024



Copyright: © 2024 by the authors. Licensee MDPI, Basel, Switzerland. This article is an open access article distributed under the terms and conditions of the Creative Commons Attribution (CC BY) license (<https://creativecommons.org/licenses/by/4.0/>).

1. Introduction

Tribology is the science devoted to studies of the interactions between rubbing surfaces. It includes contact mechanics and research on friction, wear, and lubrication. Studies of contact interactions between elastic solids started from the classic works of Hertz [1,2] and Boussinesq [3]. They considered problems for solids having ideal canonical shapes, e.g., elliptical paraboloids, spheres, cones, and flat-ended cylinders. However, it was realised soon that the topography of surfaces may have a great influence on the resulting stress–strain fields, while all engineering surfaces possesses some roughness, regardless of their preparation method. The surface roughness and asperity deformations have very significant influences on friction, wear, energy dissipation during the relative sliding of surfaces, and other processes of tribology. For example, it was shown that the fatigue lives of gears with superfinished teeth, i.e., whose average roughness was reduced by a factor of 5, were about four-times greater than the lives of gears without the improved surface finish [4].

The competition “Contact Mechanics Challenge” [5] was dedicated to celebrate 50 years of the Greenwood and Williamson (GW) model [6]. This research competition was designed to test various approximate methods for solving the problem of an elastic contact between the mathematically defined fractal rough surfaces under small adhesion [5]. Although 12 international groups took part in this “contact sport of rough surfaces”, the results were not very impressive. The formulation of the task and the outcomes of the competition raise doubts about their correctness: “this is disappointing as friction has been studied since the times of Leonardo and in 500 years, no predictive model has emerged, nor any significant improvement from rough contact models” [7]. Thus, although no convincing models so far

have been presented, the international scientific community realises that proper statistical approaches to surface roughness and modelling of contact between the surfaces are of great practical interest, not only for the dry friction phenomenon, but also for almost all areas of modern tribology. Here, we discuss various attempts to characterise real surfaces by some statistical parameters or by various statistical models of rough surfaces. We also discuss some standard parameters of roughness, surfaces having a Gaussian distribution of asperity heights, along with models that are based on the fractal assumptions or attempts to model rough surfaces by their power spectral density (PSD). As Carpick has correctly noted, “For more realistic rough surfaces, the problem becomes a multiscale exercise in surface-height statistics, even before including complex phenomena such as adhesion, plasticity, and fracture” [8].

The term multiscale analysis has many rather different meanings. Usually, multiscale asymptotic analysis is applied to systems that may be separated to subsystems whose components have specific features at multiple temporary and/or spatial scales. If the components or variables of the systems vary on different time or space scales, then it is often convenient to introduce the so-called fast–slow or large–small variables. The introduction of such variables enables the researchers to reduce the problem formulation to problems for two or more subsystems. The multiscale analysis in application to some physical problems is often treated as the renormalisation group method, which reduces a difficult problem for a system to a sequence of simpler problems for separated scales. Multiscale approaches are used in many branches of science ranging from Kolmogorov’s multiscale approach to turbulent eddy cascade [9] to asymptotic analysis of space-periodic steady convective magnetic dynamos in a rotating layer of incompressible electrically conducting fluid [10]. As A. Chorin wrote in his Foreword to Barenblatt’s book [9], “We are at the beginning of the age of multiscale science and multiscale computation, with a growing need to understand not only phenomena on each of many scales but also the interaction between phenomena at very different scales”.

Here, the term “scale” is related to the capabilities of the system to involve a different physical/chemical mechanism of interaction between surfaces at each specific scale. The model scale depends on the characteristic length under investigation, and it depends also on the processes involved in interactions between surfaces. For example, the atomic scale is responsible for chemical interactions (if any), the nanoscale asperities are mainly responsible for molecular adhesion, and the microscale asperities are related to the mechanical interlocking of surface protuberances and their plastic deformations. If two or more mechanisms of interaction are involved in the model, then the model is a multiscale one. This review does not intend to describe only recent results in the field of the analysis of rough surfaces, but rather, it intends to provide a critical evaluation of key papers having a crucial influence on engineers working in the area of tribology. We present a new look at the papers that are customarily considered as the classic ones. We critically analysed these papers and analysed some of the common misinterpretations of these paper that may be considered as myths. Therefore, we refer to the original papers and not to recent papers, which just repeat the common mistakes.

2. Preliminaries, Scales, and Levels of Surface Roughness

Questions related to the modelling of rough surfaces have been intensively studied; see, e.g., the fundamental monograph by Whitehouse [11] and the references therein. In spite of many attempts to involve surface topography in the problems of tribology, up to now, there is no clear understanding of how roughness affects contact and dry friction phenomena.

The scale of consideration of any tribological problem is very important. For example, further development of micro-/nanotechnologies requires studies of surfaces whose asperities are at the nano-/molecular scale. Roughness has a crucial influence on the dry friction phenomenon when liquid lubricants are not used, e.g., for nano-/microscale devices and devices used in a vacuum environment. The tribological properties of macro-mechanical objects may differ by many orders of magnitude from the properties of nanoscale objects.

The following distinctions between the scales l may be introduced [12]: (i) the atomic scale reflects the phenomena specific to the characteristic length $l \leq 1$ nm, in particular chemical interactions between surfaces; (ii) the nanoscale reflects phenomena specific to the characteristic length $1 \text{ nm} \leq l \leq 1 \text{ }\mu\text{m}$, mainly the van der Waals interaction between surfaces; (iii) the microscale is specific to the characteristic length $1 \text{ }\mu\text{m} \leq l \leq 1 \text{ mm}$, namely the mechanical interlocking of asperities or their plastic deformations.

The nanoscale has several specific features. For example, studying the asperities of crystalline materials, one has to take into account the Polonsky–Keer effect: “when asperity size decreases and becomes comparable to the characteristic microstructural length, contact plastic deformation becomes increasingly difficult, and finally impossible”. Hence, “below a certain threshold asperity size, the microcontact response becomes purely elastic” [13,14].

Another very important feature of real surface roughness is its multilevel nature. In 1957, Archard argued that real roughness has a hierarchical multilevel structure and presented an iterative procedure of the model construction [15]. In fact, he considered a spherical punch of radius R_0 that was covered by small spherical asperities of radius R_1 superimposed on the initial sphere. In turn, the latter set of asperities was covered by the next generation of spherical protuberances of radius R_2 , and so on. Note that the Archard construction leads to a number of overlapping regions, and hence, it was noted [16] that the Archard profile is not a self-similar fractal, contrary to the statement of Greenwood and Wu [17].

Let us specify our terms. The model is hierarchical if its vertical construction consists of several generations of asperities. The question of whether a surface topography may be specified as multilevel is related to the surface structure and to whether the asperities of the m -th generation are located at the same height or not. If all asperities of the same generation are located at the same height, then it is a single-level model, even if it was a multiscale model, i.e., the configuration of the model would allow the single-level asperities to be engaged in the mechanisms of the interactions between surfaces specific to at least two length scales. If the location heights of the same-generation asperities vary, then it is a multilevel model. For example, the C_B profile introduced by one of the authors (F.B.) [16,18] and some modifications of the profile (see, e.g., [19–21]) are single-level models, while the profile introduced by Borodich and Onishchenko [22,23] is a multilevel model.

It is interesting to note that, although the statement that the roughness or attachment devices of animals exhibit a multilevel hierarchical structure is currently widely accepted, and it is attributed to the findings by S. Gorb (Kiel University) and his colleagues [24], along with other experts in the biology of animals [25], the Archard concept of a hierarchical multilevel “bump on bump” or “protuberances on protuberances on protuberances” structure of surface roughness remained largely undeveloped until 1993 when Borodich and Onishchenko [22] introduced the multilevel hierarchical model of roughness.

The Archard concept was employed in numerical simulations of friction between a rough surface and a nominally flat slider that was represented as a multiscale, hierarchical system of connected deformable components [12]. The friction force has been calculated as the ratio between dissipated energy $U_{dissipated}$ and sliding distance x . The assumption of the vacuum environment allowed reducing the energy dissipation to three sources: (i) breaking of metallic bonds, which corresponds to the atomic scale ($U_{chemical}$); (ii) breaking of van der Waals bonds, which corresponds to the nanoscale (U_{vdW}); and (iii) mechanical interlocking of asperities at the microscale ($U_{mechanical}$), i.e.,

$$F_f = \frac{U_{chemical} + U_{vdW} + U_{mechanical}}{x}.$$

In this case, the friction coefficient μ can then be expressed as $\mu = U_{dissipated} / (P + A)$, and it can be split into several components attributed to the mechanism of energy dissipation [26]. Here, P is the normal force and A is the force of adhesion.

Because the elastic components of the slider of different scales are coupled, a deformation of any asperity of the model causes deformations of the whole system, i.e.,

the assumptions that the asperities act independently was not used. In this model, the Polonsky–Keer effect [13,14] was taken into account in application to nanoscale asperities for the first time. This effect is the reason that the atomic-/nanoscale asperities do not have plastic deformations even under very high pressure.

3. Early Methods of Roughness Characterisation and Contact Problems for Rough Surfaces

Let us consider a solid that nominally occupies a negative half-space $z \leq 0$. We use the Cartesian x, y, z coordinates. The solid is bounded by a nominally flat rough surface. Take a plane $y = 0$ perpendicular to such a surface, then the cross-section between the surface and the plane is referred to as a surface profile or a roughness profile $z(x)$. The origin (O) of the Cartesian coordinates x, y is at the point of initial contact between the Atomic Force Microscope (AFM) or the stylus probe and the surface. We will consider profiles of nominal length L or $2L$.

Let \bar{z} denote the mean profile line, i.e.,

$$\frac{1}{2L} \int_{-L}^L [z(x) - \bar{z}] dx = 0,$$

where $2L$ is the nominal length of the profile, i.e., the length of projection of the profile on the boundary plane.

In practice, we measure the roughness at equidistant points x_1, x_2, \dots, x_n , where $x_1 = 0$. Evidently, $\bar{z} = 0$ due to the choice of the origin of the coordinate system.

3.1. Some Popular Statistical Parameters of Roughness

Let us introduce the density probability function $\phi(z)$, which shows the probability that the height $z(x)$ at a surface point x is between z and $z + dz$. The right-tailed cumulative distribution function of the surface heights $\Phi(z)$ is defined as

$$\Phi(z) = \int_z^\infty \phi(t) dt.$$

In 1933, Abbott and Firestone [27] suggested to calculate the total length of the slice of the profile above the level $z = h$ and equating this length to $\Phi(h)$. Apparently, this was the first use of statistical tools in application to surface roughness. In tribology, this function is called the Abbott–Firestone, Abbott, or bearing area curve.

After the Abbott–Firestone curve was introduced, there was a period that was characterised by Whitehouse [28] as, “the parameter rash”, because a huge number of statistical parameters of roughness were introduced. These characteristics were related to the vertical distribution of heights, the horizontal distribution of the rough profiles, and the shapes of asperities [29]. Apparently, the most popular height parameter is the maximum height R_{max} of the profile $z(x)$ defined on an interval $[-L, L]$, which is defined as

$$R_{max} = \max_{x \in [-L, L]} z(x).$$

The arithmetical mean deviation of the surface R_a and the root-mean-squared (rms) height R_q are also very popular parameters of surface roughness:

$$R_a = \frac{1}{2L} \int_{-L}^L |z(x)| dx \approx \frac{\sum_{i=1}^n |z(x_i)|}{n}, \quad R_q = \left[\frac{1}{2L} \int_{-L}^L [z(x)]^2 dx \right]^{1/2},$$

where n is the number of points of measurements on the interval and $z(x_i)$ is the measured height at the interval point x_i . Note that R_q is the square root of the mean-squared deviation with respect to the mean profile line $\bar{z} = 0$.

More than 30 statistical parameters of roughness are currently in use [29]. In spite of these attempts, there is no clear understanding of how these parameters affect contact

and friction. This situation may confuse practical engineers because the engineers should follow the standards, while the European and British standard [30] contains over 20 surface and profile parameters. The situation is worse in the American standard [31] because the local engineers followed the fashion to use the so-called fractal terminology and they included in the standard not only all parameters of the European standard, but also many additional parameters, including procedures for the evaluation of surface topography using the fractal parameters.

Although some statistical parameters of roughness, e.g., the Abbott–Firestone curve, may be quite useful for specific engineering purposes, most of them are rather useless [28].

3.2. Contact Problems for a Thin Elastic Layer

The Abbott–Firestone curve is a quite useful parameter that may be correlated with the contact properties of the rough surfaces. For example, consider a rough punch that contacts a soft thin elastic coating on a hard elastic half-space. It is known (see, e.g., [32,33] and the references therein) that, if the characteristic size of the contact region is larger than the layer thickness, then the leading term of the asymptotic solution may be represented as the contact between the punch and the Fuss–Winkler foundation, which is also known as the spring bed mattress elastic foundation [34]. If the half-space is rigid and E and ν denote, respectively, the elastic modulus and Poisson’s ratio of the layer, then the spring constant k of the Winkler–Fuss spring layer is

$$k = \frac{E(1 - \nu)}{h(1 + \nu)(1 - 2\nu)}.$$

In this case, the compressing force is

$$P(\delta) = kV(\delta),$$

where $V(\delta)$ is the volume of the body under the cross-section of height $z = \delta$.

3.3. Zhuravlev and Kragelsky Models of Contact between Rough Elastic Surfaces

In 1940, Zhuravlev presented a statistical model of contact between rough surfaces [35,36]. It was assumed that spherical asperities of the same radius R have various heights, and therefore, their number at a specific height ζ increases as the level of consideration goes deeper into the rough surface.

Assuming the distribution of the summits of the asperities at various levels ζ of a surface element are characterised by a function $\phi(\zeta)$ (the same for both surfaces) and employing the Hertz contact model for each asperity, he wrote the general relation between the contact force P and the area A of true contact

$$\begin{aligned} P &= \frac{\sqrt{2R}}{3\pi k_1 N} \int_0^{x/2} \int_0^{x/2} [x - (\zeta_1 + \zeta_2)]^{3/2} \phi(\zeta_1) \phi(\zeta_2) d\zeta_1 d\zeta_2, \\ A &= \frac{\pi R}{2N} \int_0^{x/2} \int_0^{x/2} [x - (\zeta_1 + \zeta_2)] \phi(\zeta_1) \phi(\zeta_2) d\zeta_1 d\zeta_2, \end{aligned} \tag{1}$$

where x is the relative compressing displacement of contacting surfaces, N is the total number of asperity summits situated at various levels of the nominal unit element of contacting surfaces from the highest summit to the level of depth x , $k_1 = (1 - \nu^2)/\pi E$, ν is the Poisson ratio, and E is the Young modulus of the material. It was shown that, if $\phi(\zeta)$ is linear, then analytical integration of the expressions (1) is quite easy and $A \sim P^{10/11}$.

In 1948, Kragelsky [37] developed the statistical approach of Zhuravlev and modelled contact and friction between two surfaces having different roughness. Instead of spherical asperities, he considered asperities as a number of rods at various heights based on a rigid plane. He argued that his model gives qualitatively the same results as the Zhuravlev one. He noted that roughness may have a Gaussian distribution of heights; however, the use of this distribution would necessarily lead to numerical integration of general expressions.

Hence, for the demonstration of the model applications, he used only linear function $\phi(z)$, as Zhuravlev did.

3.4. The Greenwood and Williamson Contact Model

The Greenwood and Williamson (GW) model [6] is based on the same assumptions as the Zhuravlev one; however, they developed the model considerably by studying also plastic deformations of asperities. In addition, as Greenwood noted [38], the Greenwood and Williamson model, “improves on Zhuravlev by assuming a Gaussian height distribution (still of identical spherical caps)”. In fact, the calculations were performed not for a Gaussian height distribution, but rather, for an exponential distribution of the sphere summits.

We need to comment that, for processes at the nanoscale, the improvements of the Zhuravlev model by Greenwood and Williamson are rather imaginary. Indeed, the nanoscale asperities do not deform plastically due to the Polonsky–Keer effect, while the height distribution of asperities is often non-Gaussian.

The use of the Zhuravlev–Greenwood–Williamson-type models assumes that the radius of the summits of surface asperities is known. If the roughness is isotropic, then the surface roughness $z(x, y)$ is characterised by just a profile $z(x)$. If the profile heights $z_m = z(x_m)$ are measured with a regular stylus or AFM step τ , i.e., one observes z_m , then the curvature (κ) of a protuberance z_m can be defined as

$$\kappa = -(z_{m-1} + z_{m+1} - 2z_m) / \tau^2$$

where $z_{m-1}, z_{m+1} < z_m$ [39]. Whitehouse and Archard [40] found that different sampling intervals gave different mean curvature, i.e., the mean curvature is a scale-dependent parameter.

4. Surface Topography as a Realisation of a Gaussian Process

In addition to attempts to characterise the roughness of nominally flat surfaces by the selection of several roughness parameters, there are very popular models of surface topography as realisations of random processes. A core assumption underlying most of these models is the normality (Gaussian distribution) of asperity heights, either explicitly stated or implied.

Models considering roughness as realisations of Gaussian (normal) processes are well established. The vast majority of research employing statistical methods for surface roughness description relies on the assumption that asperity heights follow a Gaussian distribution. A Gaussian surface is completely defined by two parameters, a mean and a covariance function $K(\delta)$ [40,41]:

$$K(\delta) = \lim_{T \rightarrow \infty} \frac{1}{2T} \int_{-T}^T [z(x + \delta) - \bar{z}][z(x) - \bar{z}] dx = \langle [z(x + \delta) - \bar{z}][z(x) - \bar{z}] \rangle.$$

The function $K(\delta)$ measures the statistical dependence of the height values of roughness at two points separated by the distance δ and, therefore, influences the horizontal distribution of the asperities of a rough surface profile. Indeed, one needs to specify both the vertical and horizontal distributions because, as was clearly formulated by Maugis [42], two profiles may have the same height and peak height (local extrema) distributions, but they may differ in the horizontal behaviour. Instead of $K(\delta)$, one can use its Fourier transform, the power spectral density (PSD) $G(\omega)$ of the signal frequency ω :

$$G(\omega) = \frac{2}{\pi} \int_0^\infty K(\delta) \cos \omega \delta d\delta.$$

The idea to model rough surfaces as such surfaces may be traced back to Linnik and Khusu [43,44] and Whitehouse and Archard [40]. In fact, Linnik and Khusu suggested to describe surface roughness using graphs of a stationary Gaussian random process having a covariance function [43]:

$$K(x) = K(0) \cdot e^{-\alpha|x|},$$

where $K(0)$ and α are the parameters of the roughness.

Various mathematical properties of Gaussian (normal) surfaces were intensively studied (see, e.g., [41,45] and the references therein). Many researchers studied non-adhesive contact problems for surfaces having Gaussian roughness (see, e.g., [42,46,47]), while several models of adhesive contact between such surfaces were developed by Fuller, Tabor, and Galanov [48–51]. However, to use these models, one needs to demonstrate that the surface roughness follows a Gaussian distribution. Unfortunately, the tools developed for Gaussian surfaces are often used without proper justification in application to surfaces whose height distribution is non-normal.

There exist various tests of normality of experimental data [52]. The most popular tests of normality are the Kolmogorov–Smirnov (KS), Lilliefors (LF), Shapiro–Wilk (SW), Anderson–Darling (AD), Cramer–von Mises (CVM), Pearson, and Shapiro–Francia (SF) ones. Our statistical analysis of grinding surface roughness showed that the distribution is not normal, either at the micro- or nanoscale [53]. The height distribution is normal for polishing papers with nominal asperity sizes of 0.3, 1, 3, 9, and 12 μm [54]. The roughness of carbon-based coatings deposited by direct current pulsed magnetron sputtering was normal at the microscale and at the nanometre scale, when AFM measurements were taken with 117 nm steps, while the same surface measured with the 10 nm AFM steps showed that the roughness of the non-biased sample was not normal [55]. Thus, there are many cases when the models developed for Gaussian surfaces are not applicable.

5. Models of Roughness Based on the Use of Fractal or PSD Concepts

The concept of “fractals” is often used in various applications. Many researchers believe that they understand the concept very well. However, their belief is usually based on the consideration of self-similar sets such as the von Koch curve, the Sierpinski carpet, or the Cantor discontinuum, i.e., the sets that are described in the book for Russian teenagers published by Vilenkin in 1965 [56]. The difficulty of studying fractals is caused by the rather vague description of the subject introduced by Mandelbrot [57]. As Greenwood commented on the situation: “Mandelbrot is somewhat reluctant to define ‘fractals’ or ‘fractal dimension’ preferring to offer examples” [39]. This is true (see, e.g., [58]). The lack of established definitions has led to the situation that the papers dedicated to fractal analysis of applied problems are often based on the repetition of common myths about fractals, which are uncritically reported in a number of papers. As we have mentioned earlier [59], the state-of-the-art approach is replaced by the state-of-the-street one or, in another words, by the vulgar fractal approach.

There are many papers trying to model roughness using fractal language. It is argued here that the researchers should avoid the fractal approaches at least in application to problems of tribology because these approaches do not have rigorous mathematical support and they suffer from the lack of clear definitions of the main concepts. In addition, during the last couple of decades, many papers have been published that tried to model rough surfaces by their power spectral density (PSD). Unfortunately, the overwhelming majority of these papers are just some interpretations of the fractal approaches. Hence, papers based on the employment of fractal or PSD approaches are considered together here because they share the same drawbacks.

5.1. The Weierstrass–Mandelbrot Function

The use of fractal concepts in tribology is due to the comment of Berry and Hannay [60] on the results by Sayles and Thomas [61], who observed the power-law behaviour of the scaled PSD of many real surfaces. Later, Berry and Lewis published a very popular paper [62], where they studied in detail the Weierstrass function modified by Mandelbrot [57]. They called this function W of complex variable t :

$$W(t; p) = \sum_{n=-\infty}^{\infty} p^{(D-2)n} (1 - e^{ip^n t}) e^{i\phi_n}, \quad 1 < D < 2, \quad p > 1,$$

the Weierstrass–Mandelbrot (W-M) function. Here, p is a parameter and ϕ_n are arbitrary phases that can be chosen so that W exhibits either deterministic or stochastic behaviour. D is equal to the box-counting (fractal) dimension of the graph of $W(t)$. They also considered the real part of the W-M function with $\phi_n = 0$:

$$W_1(x; p) = \sum_{n=-\infty}^{\infty} p^{(D-2)n} (1 - \cos p^n)x, \tag{2}$$

A paper by Majumdar and Bhushan [63], which had a big impact on the tribology community, suggested to measure the PSD of a real rough surface and replace studying the surface by studying a truncated W-M function:

$$\tilde{W}_1(x; p) = \Lambda^{(D-1)} \sum_{n=n_1}^{\infty} p^{(D-2)n} \cos 2\pi p^n x, \quad 1 < D < 2, \quad p > 1, \tag{3}$$

having the same PSD. The integer number n_1 corresponds to the low cut-off frequency of the profile, and Λ is the so-called characteristic length scale of the profile.

The first papers where contact problems were studied for fractal-shaped indenters were published in 1991 [18,64]. In [18], the C_B profile was introduced, and the model has been discussed above. The model of elastic–plastic contact presented by Majumdar and Bhushan (M-B) employed the fractal W-M function (3). Borodich argued that the M-B model’s assumptions are controversial and the M-B model exhibits inherent flaws. Indeed, the model employs of superposition of the solutions of the nonlinear Hertz-type contact problems with non-fixed contact regions. Evidently, one cannot decompose the W-M function and use such superposition; nevertheless, it was used by many authors (see, e.g., [64,65]). In addition, the Hertz approach is not applicable to their model because the ratio of the contact radius to the radius of the asperity goes to infinity as the number of generations of the prefractal increases [66]. Although this M-B model was withdrawn by Bhushan, who wrote that, he, “now finds that any fractal characterisation model including M-B model does not give unique values of fractal parameters” for roughness [67] and “the fractal approach is not practical for engineering surfaces” [68], it is still very popular and it is discussed by many researchers.

5.2. Mathematical and Physical Fractals

Studying fractal approaches to solid mechanics, one of the authors (F.B.) realised that one should clearly distinguish mathematical and physical fractals [69]. Although both kinds of fractals use the concept of a cover of the object (surface) by cubes or spheres of some size δ , they are fundamentally different. Indeed, mathematical fractals are studied considering limits for $\delta \rightarrow 0$, while physical fractals have to demonstrate a kind of power-law behaviour in some interval between the lower δ_* and upper Δ_* cut-offs.

5.2.1. Some Features of Mathematical Fractals

Graphs of mathematical fractal curves are nowhere differentiable. Any part of a rough profile modelled as a mathematical fractal has infinite length. Hence, one cannot use such concepts as the surface energy or work of adhesion, and one can only use the concept of the energy attributed to a unit of fractal measure [70].

One cannot use the concepts of tangential and normal vectors for a solid having a fractal boundary. Even to formulate and prove the Gauss–Ostrogradsky theorem, one needs to use quite sophisticated mathematical tools [71].

It has been proven that the box-counting (Minkowski) fractal dimension of the W-M function graph (2) is equal, D , while nobody could calculate the Hausdorff (Hausdorff–Besicovitch) dimension of the graph. Hence, it is difficult to understand the statement [72] that “for the Gaussian-based models that we have in mind, all the common definitions are applicable, and all produce the same numerical value for the dimension”.

Thus, modelling of surface roughness by a mathematical fractal translates the difficult problem of tribology to the more difficult problem of mathematical physics.

5.2.2. Limits of Physical Fractal Description of Roughness

Although it was often claimed that the fractal dimension is a scale-independent or scale-invariant parameter of roughness (see, e.g., [18,64]), this is not true. A research group from the Hebrew University of Jerusalem analysed data published in *Physical Reviews* journals. They showed that the so-called fractal behaviour spreads usually for just 1.5 orders of magnitude [73,74]. Mandelbrot disagreed with the conclusion of the Jerusalem group; he said that the prevalence of published examples demonstrating power-law correlations in tribology research might be attributable, in part, to an over-enthusiasm for the PSD approach, potentially exacerbated by limitations in the peer-review process [75]. However, the group insisted that limited-range relations for physical fractals dominate observations in Nature [76]. If the FD value remains stable for less than two or three orders of magnitude, the fractal approach becomes impractical, as Whitehouse pointed out [77]. Indeed, in this case, if the lower cut-off of the observed power-law behaviour of roughness is, say, $\delta_* = 10$ nm, then the upper cut-off is just $\Delta_* = 310$ nm, and one needs to use another model for microscale roughness.

5.3. Parametric–Homogeneous Rough Surfaces

One can understand better the properties of the W-M function employing the theory of parametric–homogeneous (PH) functions introduced and developed by Borodich [78–80]. In fact, applications of the concept to contact problems was discussed at ICTAM in Haifa in 1992 [81]. In particular, the concept includes PH and parametric–quasi-homogeneous (PQH) functions. They are defined in the following way. The function $B_d : \mathbb{R}^n \rightarrow \mathbb{R}$ is called a PQH function of degree d and parameter p with weights $\alpha = (\alpha_1, \dots, \alpha_n)$ if there exists a positive parameter p , $p \neq 1$ such that it satisfies the following identity:

$$B_d(p^{m\alpha_1} x_1, \dots, p^{m\alpha_n} x_n; p) = p^{md} B_d(\mathbf{x}; p), \quad m \in \mathbb{Z}.$$

The PH functions B_d are the particular case of PQH functions when $\alpha_1 = \dots = \alpha_n$.

From the definition of the PQH function, one can obtain the following properties. Any PQH function of zero degree $B_0 : \mathbb{R}_+^n \rightarrow \mathbb{R}$ is an automorphic function with respect to a discrete group of quasi-homogeneous dilations $\Gamma_{p^{\alpha m}}$, where $\Gamma_{p^{\alpha m}} \mathbf{x} = (p^{m\alpha_1} x_1, \dots, p^{m\alpha_n} x_n)$.

For each $B_d : \mathbb{R}_+^n \rightarrow \mathbb{R}$, there exists a homogeneous function of degree d $H_d : \mathbb{R}_+^n \rightarrow \mathbb{R}$ and a PQH function of zero degree $B_0 : \mathbb{R}_+^n \rightarrow \mathbb{R}$ such that

$$B_d(\mathbf{x}; p) = H_d(\mathbf{x}) B_0(\mathbf{x}; p).$$

In fractal geometry, the quasi-homogeneous dilations of coordinates are usually called the self-affine dilations. The graphs of PH functions can be smooth, e.g., the log-periodic sinus functions, or they can be nowhere differentiable, in particular fractal. It can be shown that such base sets used in fractal geometry as the von Koch curve, the W-M function, and the Cantor staircase are examples of PH sets. However, in general, the fractal properties of a curve and the PH property are independent of each other.

The W-M function is a PH function of degree $d = (2 - D)$ and parameter p ; hence, the graph of $W_1(x; p)$ has a specific trend that can be described as x^{2-D} . The function is a particular example of a fractal PH function, and it cannot be considered as the general fractal model of rough surfaces.

5.4. PSD Approach to Rough Surfaces

Over the past two decades, the PSD approach has gained significant traction within the tribology community (see, e.g., [82,83]). In fact, the authors of the papers have focused solely on the PSD to characterise rough surfaces in tribology.

It was noted that quantities varying with time have often fractal graphs, and one way in which their fractal nature is manifested is by a power-law behaviour of the covariance function $K(x)$ [84]. This note was misinterpreted in many papers, which assumed that, if $K(x)$ and, respectively, $G(\omega)$ have power-law behaviour, then the graph or profile is fractal. For example, Persson [83] states that the power spectrum of a self-affine fractal surface is $G(\omega) \sim \omega^{-2(H+1)}$, where H is the Hurst exponent and H is related to the fractal dimension as $D = 3 - H$.

Actually, one can find the last statement in many other papers, i.e., it is often assumed that the scaling properties of rough surfaces are defined by the exponent H (the Hurst exponent), and the fractal dimension D of the surface or a profile can be calculated as $H = E - D$. Here, E is the Euclidean dimension of the space: $E = 3$ for a surface and $E = 2$ for a curve. This is usually explained by an example saying that, under quasi-homogeneous scaling of coordinates $x \rightarrow \lambda_1 x$ and $y \rightarrow \lambda_2 y$, the fractal surfaces appear as approximately the same or

$$x \rightarrow \lambda x; \quad z(x) \rightarrow \lambda^H z(x).$$

Here, $\lambda_1 = \lambda > 0$ and $\lambda_2 = \lambda^H$ are scaling factors. Using the above-mentioned properties of PQH and PH functions, one can construct a function having an arbitrarily given box-counting fractal dimension D and an arbitrarily given trend x^H , $H > 0$ (see the examples in [78,79]). Hence, the term Hurst exponent is ill-defined and the statement that the fractal dimension $D = E - H$ is not correct.

5.5. Some Counterexamples to Popular Statements of Fractal and PSD Approaches

5.5.1. PSD of Some Smooth PH Functions

Let us show that the connections of the fractal dimension and the slopes of PSD functions in logarithmic coordinates are meaningless. Let us show that some functions having smooth graphs may have a power-law PSD. Consider a smooth PH uncton, namely a sin log-periodic function. Figure 1 shows the power spectra for $z(x) = \sin(2\pi \ln(x) / \ln(p))$ with $x \in [0.0001, 1]$.

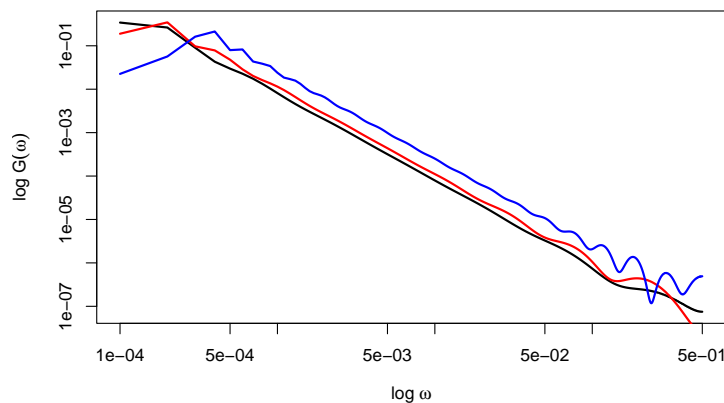


Figure 1. The power spectra of the profile $z(x) = \sin(2\pi \ln(x) / \ln(p))$ for $x \in [0.0001, 1]$ with $p = 3.5$ (black), $p = 2.5$ (red), and $p = 1.5$ (blue).

Although the function itself is not fractal, its power spectrum exhibits a linear trend on a logarithmic scale within a specific range.

5.5.2. PSD Does Not Describe the Contact Properties of Surfaces

Using rather vague arguments, Persson represented the diffusion of stress fields in a solid contacting with a rough counterpart using the diffusion equation [85]. Criticising the Persson approach [85], Borodich [86] wrote that two punches with identical fractal surface textures can exhibit distinct asymptotic behaviours in their load–displacement relationships, depending on whether they are positioned above or below the surface. Then,

it was shown [53] that any surface and its replica have the same PSD; therefore, it is not sufficient on its own to fully characterise the contact properties of rough surfaces. In spite of this critique, this erroneous approach has been multiplied in a number of papers; see, e.g., [87].

Let us demonstrate this by simple examples. A rough surface has asperities and valleys that can be schematically considered as pins whose tips are directed up and down (Figure 2a). If the surface was polished, then the asperities (the pins whose tips are directed up) were removed (Figure 2b).



Figure 2. Schematic representations of surfaces: (a) up (asperities) and down (valleys) pins; (b) down pins (asperities were removed).

Now, let us consider a solid that is described by the fractal Mandelbrot function. It is evident that, for the tribological effect of contact between the solid and the intact rough surface having sharp asperities, the pins whose tips are directed up (Figure 3a) and the polished surface that is the replica of the former one (Figure 3b) will be rather different. However, the PSD of the former and the latter surfaces are the same. As a Russian poet S. Marshak wrote ironically about a philosopher [88], “The world,” he taught, “is my representation!”. When his son stuck a pin under the seat of his chair, he cried out, “Horror! How terrible is my representation!” Thus, the rough surfaces cannot be represented solely by the PSD.

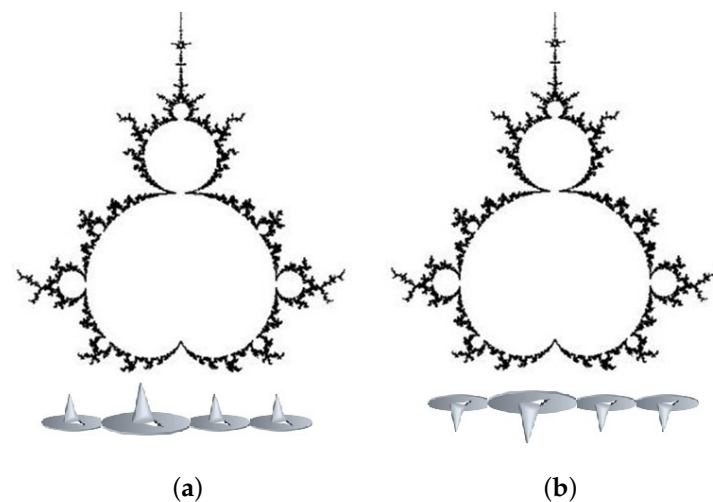


Figure 3. Schematic representations of contact between a fractal solid and two surfaces: (a) up and down pins; (b) down pins (a polished surface).

5.5.3. PSD of Truncated Weierstrass–Mandelbrot Functions

Now, we demonstrate that the slopes of the PSD for different truncated Weierstrass–Mandelbrot functions are almost the same.

Let us consider two truncated Weierstrass–Mandelbrot functions:

$$C_t(x; p) = \sum_{n=-N}^N p^{-(2-D)n} (1 - \cos(p^n x)), \quad A(x; p) = \sum_{n=-N}^N (-1)^n p^{-(2-D)n} \sin(p^n x),$$

where N is a large natural number, $p > 1$, and $D \in (1, 2)$. In addition, let us consider a function $x^{D-2}C_t(x; p)$. If $N \rightarrow \infty$, then $C_t(x; p) \rightarrow C(x; p)$ and D is their box dimension; however, they have different trends.

Let us fix the values $p = 1.6$ and $D = 1.6$ and vary N . The PSDs for these functions can be calculated numerically and are presented in logarithmic coordinates in Figure 4.

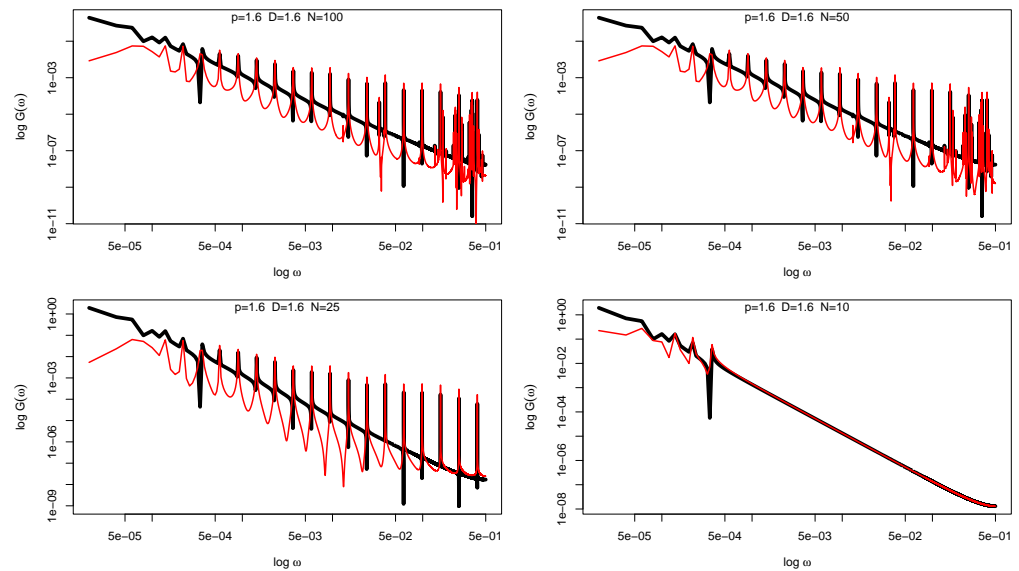


Figure 4. The power spectra of the profile $C_t(x; p)$ (black) and the profile $x^{D-2}C_t(x; p)$ (red) for $x \in [0, 1]$ with $p = 1.6$, $D = 1.6$, and $N = 10, 25, 50, 100$.

One can see that the average PSDs are approximately the same, while the functions are rather different.

Now, let us fix the values $p = 1.6$ and $N = 100$, vary D , and numerically calculate the PSD for the obtained functions. The results are presented in logarithmic coordinates in Figure 5.

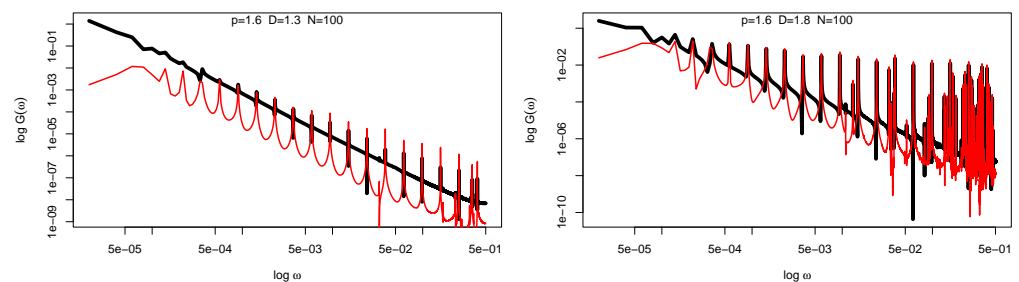


Figure 5. The power spectra of the profile $C_t(x; p)$ (black) and the profile $x^{D-2}C_t(x; p)$ (red) for $x \in [0, 1]$ with $p = 1.6$ and $N = 100$ for $D = 1.3$ (left) and $D = 1.8$ (right).

Note that, for $N = 100$, the graphs of $C_t(x; p)$ and $x^{D-2}C_t(x; p)$ are very close to the graphs of the PH functions of degrees $d = 2 - D$ and $d = 0$, respectively. We know that these functions have the same D and different trends (see the discussion above), while the slopes of their PSDs are almost equal.

The same procedure we have outlined can be directly applied to analyse $A(x; p)$ and $x^{D-2}A(x; p)$. The PSDs for these profiles are shown in Figure 6.

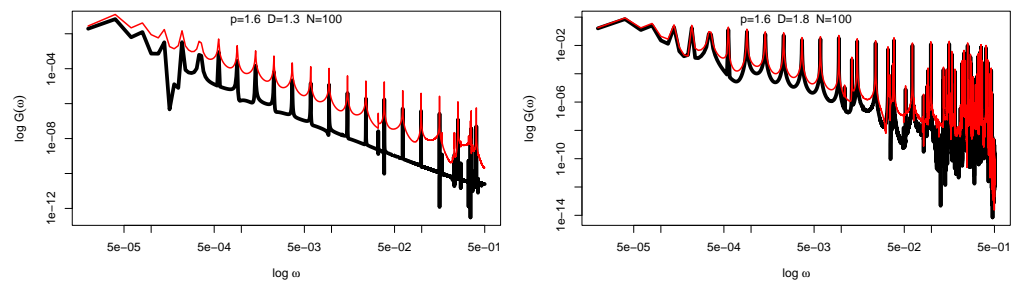


Figure 6. The power spectra of the profile $A(x; p)$ (black) and the profile $x^{D-2}A(x; p)$ (red) for $x \in [0, 1]$ for $x \in [0, 1]$ with $p = 1.6$ and $N = 100$ for $D = 1.3$ (left) and $D = 1.8$ (right).

We see that to the same conclusion holds as above.

5.5.4. PSD of Polished Surfaces

As has been mentioned, enhancing the surface finish can significantly extend the lifespan of gears [4]. Considering the roughness of polished parts, Chen et al. [89] argued that, after vibratory polishing, some elements of the topography of the initial surface and the topography of the polished parts coexist in the final topography. To model the topography obtained, they discussed the Pawlus superposition method [90] and the Tang method [91]. Let us use some ideas of the Pawlus superposition method. Let an intact surface be described by a realisation $f_1(x)$ of a Gaussian process. Let us assume that the topography of polished parts is described by $0.1f_2(x)$, where the profile $f_2(x)$ is a realisation of another Gaussian process. Hence, the fully polished surface is described by $f_3(x) = \min[f_1(x), 0.1f_2(x)]$, shown in Figure 7.

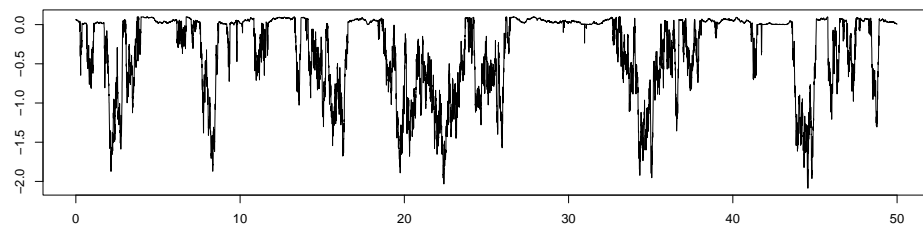


Figure 7. The “polished” profile $f_3(x) = \min[f_1(x), 0.1f_2(x)]$, where the profiles $f_1(x)$ and $f_2(x)$ are realisations of independent Gaussian processes.

Figure 8 shows the power spectra for the profile $f_1(x)$ (black), the profile $f_2(x)$ (red), and the “polished” profile $f_3(x) = \min[f_1(x), 0.1f_2(x)]$ (blue).

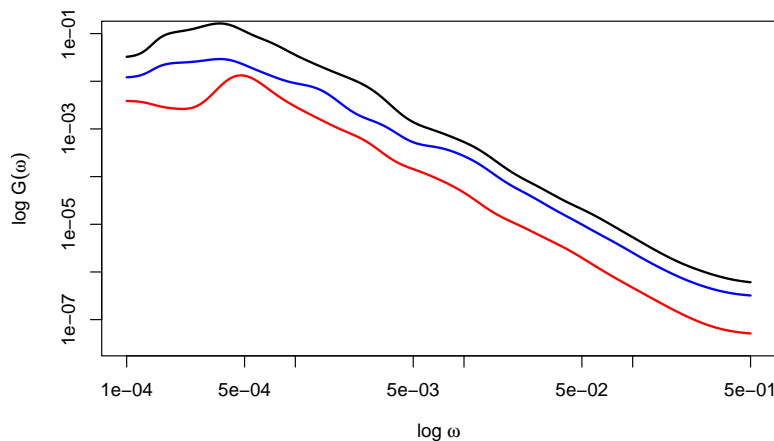


Figure 8. The power spectra for the profile $f_1(x)$ (black), the profile $f_2(x)$ (red), and the “polished” profile $f_3(x) = \min[f_1(x), 0.1f_2(x)]$ (blue).

These three surface profiles, despite exhibiting distinct appearances and tribological properties, surprisingly share the same exponent of 1.95 in their power spectra, i.e., $G(\omega) \sim 1/\omega^{1.95}$. Thus, the slope of the power spectral density alone is not sufficient to characterise the tribological properties of polished surfaces.

6. Statistically Justified Descriptions of Surface Roughness

The process of mimicking a real surface in order to create a synthetic surface is called the surface synthesis. Synthesised surfaces offer tremendous value to tribology researchers. By enabling the creation of surfaces with controlled properties, they allow for the modelling and investigation of various tribological phenomena, such as friction, wear, etc. [92]. It is assumed usually that some characteristics of synthetic roughness are the same as the characteristics of the original surface. The chosen characteristics may be taken as some characteristics from the international standards [30,31], the fractal dimension of the roughness, or its PSD function. It can be also assumed that the roughness may be described by some random process, e.g., the Gaussian process. However, one has to justify that a new surface has the same statistical properties as the original one. As has been demonstrated above, these methods of surface synthesis have various drawbacks, and usually, they do not give a solid statistical support. Therefore, we will discuss a statistical approach to problems related to the synthesis of rough surfaces of solids introduced by two of the authors (F.B. and A.P.).

Similar to the notion of the representative elementary volume used in the mechanics of random inhomogeneous materials, we introduce the notion of the representative elementary pattern of roughness (REPR) and the statistically representative pattern of surface roughness (SRPSR). The REPR is the smallest interval (or area) of a rough surface that statistically represents the whole surface. Hence, from a statistical point of view, the REPR cannot be distinguished from the original rough surface. For patterns smaller than the REPR, a representative property cannot be obtained. Indeed, the Kolmogorov–Smirnov (K-S) statistic is a nonparametric goodness-of-fit test, which may be used to determine whether two distributions differ, i.e., the K-S statistic may test whether a given set of data (its empirical distribution) deviates significantly from a hypothesised reference distribution or another set of data. The K-S statistic provides a solid statistical support to the described method and enabled us to extract the REPR of the surfaces. This will enable us to synthesise simpler surfaces with equivalent roughness in terms of the height distribution.

The employment of some statistical techniques of time series analysis, e.g., the moving window technique, may be effectively used for the extraction of the REPR from the experimental data [93]. The moving window techniques are novel only for their use in tribology; however, these techniques are used in many methods of time series analysis, in particular in Singular Spectrum Analysis (SSA) methods [94]. It is known that the SSA methods may be effectively used in many areas of applied statistics, and they are not computationally demanding [95,96]. The presented algorithm for the determination of the REPR is even simpler than the SSA algorithm. The REPR algorithm has been described by the authors elsewhere [97]. It should be applied to representative sets of roughness profiles.

For the sake of simplicity, we describe it here just for one profile, which is described as heights z_1, z_2, \dots, z_N .

Take the moving window of length N_s , where $N_s < N$, and slide it along the profile. Specifically, for the starting point i , $0 \leq i \leq N - N_s$, take a subset series of heights within the sliding window $(z_{i+1}, z_{i+2}, \dots, z_{i+N_s})$.

Compute the similarity between the long series z_1, z_2, \dots, z_N of the profile and the subset sample with the shift i using the Kolmogorov–Smirnov statistic:

$$D_{N,N_s;i} = \sup_x \left| F_N(z) - F_{N_s;i}(z) \right|,$$

where $F_N(z)$ and $F_{N_s;i}(z)$ are the cumulative distribution functions for two samples, respectively.

For the fixed window of length N_s , define a subset sample that minimises the Kolmogorov–Smirnov statistic with respect to the shift i . Also, we consider the KS-based distance measure defined by

$$D_N(N_s) = \min_{i=0, \dots, N-N_s} D_{N, N_s; i}$$

as a function N_s .

Choose N_s such that the measure $D_N(N_s)$ is close to zero and N_s is not big, e.g., take N_s as the smallest integer such that $D_N(N_s) < 0.05$.

Let us consider an example. From real profilometer measurements of a cooper engineering surface of length $N = 668$, one can obtain the REPR of length $N_s = 52$, as is shown in Figure 9. As one can see, this REPR does not behave like a fractal or a realisation of a Gaussian process.

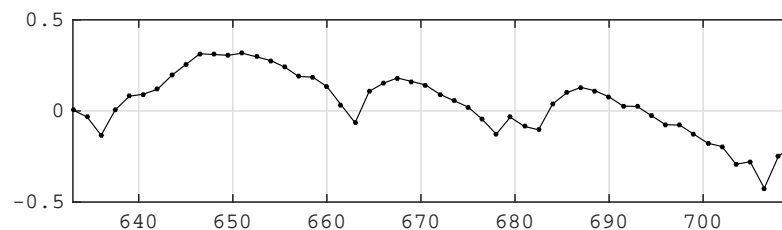


Figure 9. The REPR for the roughness data obtained by a profilometer; $N = 668$, $N_s = 52$, and $i = 423$.

However, we need to find the size of the moving window and its location such that the appropriate pattern (the SRPSR) satisfies not only the condition that it is entirely typical of the whole surface, but also it satisfies some additional conditions depending on the contact problem formulation and the numerical solver used. For example, the synthesised surface may be used by the Polonsky–Keer solver of contact problems for rough surfaces [98,99] based on the use a Fast Fourier Transform (FFT). It is known that the Fourier Transform converts a signal or a graph of a function to the frequency domain. In the case of measurements of roughness, one needs to use a discrete Fourier Transform, which is a rather slow process having complexity $O(n^2)$, where n is the number of discrete measurements. The Fast Fourier Transform (FFT) may greatly reduce the complexity of computation to $O(n \log n)$. However, the classic realisations of the FFT algorithm, e.g., the Cooley–Tukey algorithm, are usually restricted to power-of-two sizes. Hence, if the the Cooley–Tukey or a similar FFT algorithm is employed in the contact solver, then the REPR should be extended to 2^n points.

Another restriction is that the direct employment of the REPR for the synthesis of a surface may cause artificial stress singularities. For example, for a profile (i.e., in the 2D problem), to avoid stress singularities, one can request that the heights at the first point and at the last point are the same.

It is assumed that the synthetic surfaces based on the described REPR techniques will be used within the framework of various contact solvers. For example, the REPR-based method may be combined with the Polonsky–Keer algorithm, which has demonstrated its effectiveness for solving various problems of contact between rough surfaces (see, e.g., [100]).

7. Conclusions

Enhancing engineers’ ability to predict real-world tribological behaviour requires modelling the key features of rough surfaces across various roughness scales. The multiscale approach is crucial for accurately capturing the complex interactions that occur between contacting surfaces. If a tribological problem under consideration is governed by both atomic/nano- and microscale phenomena, then the synthesis of surfaces should be based on data obtained by a stylus, or white light interferometry (at the microscale) and AFM, or

confocal microscopy (at the atomic/nanoscale). The REPRs should be obtained for both sets of measurements.

Using examples, it was demonstrated that the many common statements about fractal or power spectral density function are wrong or just meaningless. Some terms are ill-defined, and papers based on the employment of the PSD and their applications to rough surfaces create just “new clothes” for the vulgar fractal approach.

It is argued that the use of two new concepts, namely the representative elementary pattern of roughness (REPR), i.e., the smallest interval (or area) of a rough surface that statistically represents the whole surface, and the statistically representative pattern of surface roughness (SRPSR) enabled us to synthesise surfaces that cannot be distinguished statistically from the original rough surfaces. To extract the REPR from the experimental data, one can use some modified statistical techniques of time series analysis, e.g., the moving window technique. Using the Kolmogorov–Smirnov statistic, one can prove that the surfaces consisting of the REPRs are statistically the same as the original surfaces.

Author Contributions: Conceptualisation, F.M.B. and A.P.; methodology, F.M.B. and A.P.; software, A.P.; validation, A.P. and X.J.; formal analysis, F.M.B. and A.P.; writing—original draft preparation, F.M.B. and X.J.; writing—review and editing, F.M.B. and X.J.; visualisation, F.M.B. and A.P.; funding acquisition, F.M.B. and X.J. All authors have read and agreed to the published version of the manuscript.

Funding: This work was funded by the National Natural Science Foundation of China (grant No. 11932004 and No. HWG2022001) and the Opening Fund of State Key Laboratory of Nonlinear Mechanics.

Data Availability Statement: The data will be made available by the authors on request.

Conflicts of Interest: The authors declare no conflicts of interest.

References

- Hertz, H. Ueber die Berührung fester elastischer Körper. *J. Reine Angew. Math.* **1882**, *92*, 156–171. [[CrossRef](#)]
- Hertz, H. On the contact of elastic solids. In *Miscellaneous Papers by H. Hertz*; Jones, D.E., Schott, G.A., Eds.; Macmillan: London, UK, 1896; pp. 146–162.
- Boussinesq, J. *Applications des Potentiels ‘a l’Étude de l’Équilibre et du Mouvement des Solides Élastique*; Gauthier-Villars: Paris, France, 1885.
- Krantz, T.L.; Alanou, M.P.; Evans, H.P.; Snidle, R.W. Surface fatigue lives of case-carburized gears with an improved surface finish. *ASME J. Tribol.* **2001**, *123*, 709–716. [[CrossRef](#)]
- Müser, M.H.; Dapp, W.B.; Bugnicourt, R.; Sainsot, P.; Lesaffre, N.; Lubrecht, T.A.; Persson, B.N.J.; Harris, K.; Bennett, A.; Schulze, K.; et al. Meeting the contact-mechanics challenge. *Tribol. Lett.* **2017**, *65*, 118. [[CrossRef](#)]
- Greenwood, J.A.; Williamson, J.B.P. Contact of nominally flat surfaces. *Proc. R. Soc. Lond.* **1966**, *A370*, 300–319.
- Ciavarella, M.; Papangelo, A. The “sport” of rough contacts and the fractal paradox in wear laws. *Facta Univ.* **2018**, *16*, 65–75. [[CrossRef](#)]
- Carpick, R.W. The contact sport of rough surfaces. *Science* **2018**, *359*, 38. [[CrossRef](#)] [[PubMed](#)]
- Barenblatt, G.I. *Scaling*; Cambridge University Press: Cambridge, UK, 2003.
- Chertovskih, R.; Zheligovsky, V. Large-scale weakly nonlinear perturbations of convective magnetic dynamos in a rotating layer. *Phys. D Nonlinear Phenom.* **2015**, *313*, 99–116. [[CrossRef](#)]
- Whitehouse, D.J. *Handbook of Surface and Nanometrology*; CRC Press: Boca Raton, FL, USA, 2011.
- Borodich, F.M.; Savencu, O. Hierarchical models of engineering rough surfaces and bioinspired adhesives. In *Bio-Inspired Structured Adhesives*; Heepe, L., Xue, L., Gorb, S.N., Eds.; Springer: Berlin/Heidelberg, Germany, 2017; pp. 179–219.
- Polonsky, I.A.; Keer, L.M. Simulation of microscopic elastic-plastic contacts by using discrete dislocations. *Ser. A Math. Phys. Eng. Sci.* **1996**, *452*, 2173–2194.
- Polonsky, I.A.; Keer, L.M. Scale effects of elastic-plastic behavior of microscopic asperity contacts. *J. Tribol.* **1996**, *118*, 335–340. [[CrossRef](#)]
- Archard, J.F. Elastic deformation and the laws of friction. *Proc. R. Soc. Lond.* **1957**, *243*, 190–205.
- Borodich, F.M.; Mosolov, A.B. Fractal roughness in contact problems. *J. Appl. Math. Mech.* **1992**, *56*, 681–690. [[CrossRef](#)]
- Greenwood, J.A.; Wu, J.J. Surface roughness and contact: An apology. *Meccanica* **2001**, *36*, 617–630. [[CrossRef](#)]
- Borodich, F.M.; Mosolov, A.B. Fractal contact of solids. *Sov. Phys.-Tech. Phys.* **1991**, *61*, 50–54.
- Plesha, M.E.; Ni, D. Scaling of geological discontinuity normal load-deformation response using fractal geometry. *Int. J. Num. Anal. Meth. Geomech.* **2001**, *25*, 741–756. [[CrossRef](#)]

20. Warren, T.L.; Krajcinovic, D. Fractal models of elastic–perfectly plastic contact of rough surfaces based on the Cantor set. *Int. J. Solids Struct.* **1995**, *32*, 2907–2922. [[CrossRef](#)]
21. Warren, T.L.; Krajcinovic, D. Random Cantor set models for the elastic-perfectly plastic contact of rough surfaces. *Wear* **1996**, *196*, 1–15. [[CrossRef](#)]
22. Borodich, F.M.; Onishchenko, D.A. Fractal roughness for problem of contact and friction (the simplest models). *J. Frict. Wear* **1993**, *14*, 14–19.
23. Borodich, F.M.; Onishchenko, D.A. Similarity and fractality in the modelling of roughness by a multilevel profile with hierarchical structure. *Int. J. Solids Struct.* **1999**, *36*, 2585–2612. [[CrossRef](#)]
24. Spinner, M.; Kovalev, A.; Gorb, S.N.; Westhoff, G. Snake velvet black: Hierarchical micro- and nanostructure enhances dark colouration in *Bitis rhinoceros*. *Sci. Rep.* **2013**, *3*, 1846. [[CrossRef](#)]
25. Gao, H.; Wang, X.; Yao, H.; Gorb, S.; Arzt, E. Mechanics of hierarchical adhesion structures of geckos. *Mech. Mater.* **2005**, *37*, 275–285. [[CrossRef](#)]
26. Borodich, F.M.; Keer, L.M. Modeling effects of gas adsorption and removal on friction during sliding along diamond-like carbon films. *Thin Solid Films* **2005**, *476*, 108–117. [[CrossRef](#)]
27. Abbott, E.J.; Firestone, F.A. Specifying surface quality: A method based on accurate measurement and comparison. *Mech. Eng.* **1933**, *55*, 569–572.
28. Whitehouse, D.J. The parameter R_a —is there a cure? *Wear* **1982**, *83*, 75–78. [[CrossRef](#)]
29. Nowicki, B. Multiparameter representation of surface roughness. *Wear* **1985**, *102*, 161–176. [[CrossRef](#)]
30. EN ISO 4287:1998+A1:2009; Geometrical Product Specification (GPS)—Surface Texture: Profile Method—Terms, Definitions and Surface Texture Parameters. ISO: Geneva, Switzerland, 2009.
31. ASME B46.1-2002; Surface Texture (Surface Roughness, Waviness and Lay). ASME: New York, NY, USA, 2002.
32. Borodich, F.M.; Galanov, B.A.; Perepelkin, N.V.; Prikazchikov, D.A. Adhesive contact problems for a thin elastic layer: Asymptotic analysis and the JKR theory. *Math. Mech. Solids* **2019**, *24*, 1405–1424. [[CrossRef](#)]
33. Kaplunov, J.; Prikazchikov, D.A.; Sultanova, L. Justification and refinement of Winkler-Fuss hypothesis. *Z. Angew. Math. Phys.* **2018**, *69*, 80. [[CrossRef](#)]
34. Johnson, K.L. *Contact Mechanics*; Cambridge University Press: Cambridge, UK, 1985.
35. Zhuravlev, V.A. On question of theoretical justification of the Amontons-Coulomb law for friction of unlubricated surfaces. *Zh. Tekh. Fiz.* **1940**, *10*, 1447–1452. [[CrossRef](#)]
36. Zhuravlev, V.A. On question of theoretical justification of the Amontons-Coulomb law for friction of unlubricated surfaces. *Proc. Inst. Mech. Eng. Part J J. Eng. Tribol.* **2007**, *221*, 893–898. [[CrossRef](#)]
37. Kragelsky, I.V. Static friction between two rough surfaces. *Bul. USSR Acad. Sci. Div. Tech. Sci.* **1948**, *10*, 1621–1625.
38. Greenwood, J.A. Surface modelling in tribology. In *Applied Surface Modelling*; Creasy, C.F.M., Craggs, C., Eds.; Ellis Horwood: New York, NY, USA, 1990; pp. 61–75.
39. Greenwood, J.A. Problems with surface roughness. In *Fundamentals of Friction*; Singer, I.L., Pollock, H.M., Eds.; Kluwer: Boston, MA, USA, 1992; pp. 57–76.
40. Whitehouse, D.J.; Archard, J.F. The properties of random surfaces of significance in their contact. *Proc. R. Soc. Lond.* **1970**, *A316*, 97–121.
41. Khusu, A.P.; Vitenberg, Y.R.; Palmov, V.A. *Roughness of Surfaces: Theoretical Probabilistic Approach*; Nauka: Moscow, Russia, 1975.
42. Maugis, D. *Contact, Adhesion and Rupture of Elastic Solids*; Springer: Berlin/Heidelberg, Germany, 2000.
43. Linnik, Y.V.; Khusu, A.P. Mathematical and statistical description of unevenness of surface profile at grinding. *Uspekhi Mat. Nauk.* **1954**, *9*, 255.
44. Linnik, Y.V.; Khusu, A.P. Mathematical and statistical description of unevenness of surface profile at grinding. *Bul. USSR Acad. Sci. Div. Techn. Sci.* **1954**, *20*, 154–159.
45. Barakat, R.; Baumann, E. Mean and variance of the arc length of a Gaussian process on a finite interval. *Int. J. Control* **1970**, *12*, 377–383. [[CrossRef](#)]
46. Nayak, P.R. Random process model of rough surfaces. *ASME J. Lub. Tech.* **1971**, *93*, 398–407. [[CrossRef](#)]
47. Nayak, P.R. Some aspects of surface roughness measurement. *Wear* **1973**, *26*, 165–174. [[CrossRef](#)]
48. Fuller, K.N.G.; Tabor, D. The effect of surface roughness on the adhesion of elastic solids. *Proc. R. Soc. Lond. A* **1975**, *345*, 327–342.
49. Fuller, K. Effect of surface roughness on the adhesion of elastomers to hard surfaces. *Mater. Sci. Forum* **2011**, *662*, 39–51. [[CrossRef](#)]
50. Galanov, B.A. Models of adhesive contact between rough elastic bodies. *Int. J. Mech. Sci.* **2011**, *53*, 968–977. [[CrossRef](#)]
51. Galanov, B.A.; Valeeva, I.K. Sliding adhesive contact of elastic solids with stochastic roughness. *Int. J. Eng. Sci.* **2016**, *101*, 64–80. [[CrossRef](#)]
52. Thode, H.C. *Testing for Normality*; Marcel Dekker: New York, NY, USA, 2002.
53. Borodich, F.M.; Pepelyshev, A.; Savencu, O. Statistical approaches to description of rough engineering surfaces at nano and microscales. *Tribol. Int.* **2016**, *103*, 197–207. [[CrossRef](#)]
54. Pepelyshev, A.; Borodich, F.M.; Galanov, B.A.; Gorb, E.V.; Gorb, S.N. Adhesion of soft materials to rough surfaces: Experimental studies, statistical analysis and modelling. *Coatings* **2018**, *8*, 350. [[CrossRef](#)]
55. Borodich, F.M.; Brousseau, E.; Clarke, A.; Pepelyshev, A.; Sanchez-Lopez, J.C. Roughness of deposited carbon-based coatings and its statistical characteristics at nano and microscales. *Front. Mech. Eng.* **2019**, *5*, 73–82. [[CrossRef](#)]

56. Vilenkin, N.Y. *Stories about Sets*; Academic Press: New York, NY, USA, 1968.
57. Mandelbrot, B.B. *Fractals: Form, Chance, and Dimension*; W.H. Freeman: San Francisco, CA, USA, 1977.
58. Mandelbrot, B.B. Fractal geometry: What is it, and what does it do? *Proc. R. Soc. Lond.* **1989**, *423*, 3–16.
59. Borodich, F.M.; Jin, X.; Pepelyshev, A. Probabilistic, fractal, and related techniques for analysis of engineering surfaces. *Front. Mech. Eng.* **2020**, *6*, 64. [[CrossRef](#)]
60. Berry, M.V.; Hannay, J.H. Topography of random surfaces. *Nature* **1978**, *273*, 573. [[CrossRef](#)]
61. Sayles, R.S.; Thomas, T.R. Surface topography as a nonstationary random process. *Nature* **1978**, *271*, 431–434. [[CrossRef](#)]
62. Berry, M.V.; Lewis, Z.V. On the Weierstrass-Mandelbrot fractal functions. *Proc. R. Soc. Lond.* **1980**, *370*, 459–484.
63. Majumdar, A.; Bhushan, B. Role of fractal geometry in roughness characterization and contact mechanics of surfaces. *J. Tribol.* **1990**, *112*, 205–216. [[CrossRef](#)]
64. Majumdar, A.; Bhushan, B. Fractal model of elastic-plastic contact between rough surfaces. *J. Tribol.* **1991**, *113*, 1–11. [[CrossRef](#)]
65. Ciavarella, M.; Demelio, G.; Barber, J.R.; Jang, Y.H. Linear elastic contact of the Weierstrass profile. *Proc. R. Soc. Lond. A* **2000**, *456*, 387–405. [[CrossRef](#)]
66. Borodich, F.M. Fractal Contact Mechanics. In *Encyclopedia of Tribology*; Wang, Q.J., Chung, Y.-W., Eds.; Springer: Berlin/Heidelberg, Germany, 2013; Volume 2, pp. 1249–1258.
67. Bhushan, B. A fractal theory of the temperature distribution at elastic contacts of fast sliding surfaces—Discussion. *J. Tribol.* **1995**, *117*, 214–215. [[CrossRef](#)]
68. Bhushan, B. *Modern Tribology Handbook*; CRC Press: Boca Raton, FL, USA, 2001.
69. Borodich, F.M. Some fractal models of fracture. *J. Mech. Phys. Solids* **1997**, *45*, 239–259. [[CrossRef](#)]
70. Borodich, F.M.; Feng, Z. Scaling of mathematical fractals and box-counting quasi-measure. *Z. Angew. Math. Phys.* **2010**, *61*, 21–31. [[CrossRef](#)]
71. Borodich, F.M.; Volovikov, A.Y. Surface integrals for domains with fractal boundaries and some applications to elasticity. *Proc. R. Soc. Lond. Ser. A* **2000**, *456*, 1–23. [[CrossRef](#)]
72. Davies, S.; Hall, P. Fractal analysis of surface roughness by using spatial data. *J. R. Statist. Soc. B* **1999**, *61*, 3–37. [[CrossRef](#)]
73. Avnir, D.; Biham, O.; Lidar, D.; Malcai, O. Is the geometry of Nature fractal? *Science* **1998**, *279*, 39–40. [[CrossRef](#)]
74. Malcai, O.; Lidar, D.A.; Biham, O.; Avnir, D. Scaling range and cutoffs in empirical fractals. *Phys. Rev. E* **1997**, *56*, 2817–2828. [[CrossRef](#)]
75. Mandelbrot, B.B. Is Nature fractal? *Science* **1998**, *279*, 783. [[CrossRef](#)]
76. Biham, O.; Malcai, O.; Lidar, D.A.; Avnir, D. Fractality in Nature—Response. *Science* **1998**, *279*, 1615–1616.
77. Whitehouse, D.J. Fractal or fiction. *Wear* **2001**, *249*, 345–353. [[CrossRef](#)]
78. Borodich, F.M. Parametric homogeneity and non-classical self-similarity. I. Mathematical background. *Acta Mech.* **1998**, *131*, 27–45. [[CrossRef](#)]
79. Borodich, F.M. Parametric homogeneity and non-classical self-similarity. II. Some applications. *Acta Mech.* **1998**, *131*, 47–67. [[CrossRef](#)]
80. Borodich, F.M.; Galanov, B.A. Self-similar problems of elastic contact for non-convex punches. *J. Mech. Phys. Solids* **2002**, *50*, 2441–2461. [[CrossRef](#)]
81. Borodich, F.M. Similarity properties of discrete contact between a fractal punch and an elastic medium. *C. R. L'Académie Sci. Ser. 2* **1993**, *316*, 281–286.
82. Persson, B.N.J. Theory of rubber friction and contact mechanics. *J. Chem. Phys.* **2001**, *115*, 3840–3861. [[CrossRef](#)]
83. Persson, B.N.J. Contact mechanics for randomly rough surfaces. *Surf. Sci. Rep.* **2006**, *61*, 201–227. [[CrossRef](#)]
84. Falconer, K.J. *Fractal Geometry: Mathematical Foundations and Applications*; John Wiley: Chichester, UK, 1990.
85. Persson, B.N.J. Elastoplastic Contact between Randomly Rough Surfaces. *Phys. Rev. Lett.* **2001**, *87*, 116101. [[CrossRef](#)] [[PubMed](#)]
86. Borodich, F.M. Comment on “Elastoplastic Contact between Randomly Rough Surfaces”. *Phys. Rev. Lett.* **2002**, *88*. [[CrossRef](#)] [[PubMed](#)]
87. Persson, B.N.J. Functional properties of rough surfaces from an analytical theory of mechanical contact. *MRS Bull.* **2023**, *47*, 1211–1219. [[CrossRef](#)]
88. Marshak, S. *Collection of Works in 8 Volumes, 4*; Khudozhestvennaya Literature: Moscow, Russia, 1969.
89. Chen, J.; Tang, J.; Shao, W.; Sun, Z.; Zhang, H.; Li, X.; Zhao, B. Numerical simulation method for three-dimensional rough surface of vibratory polishing parts. *Tribol. Int.* **2024**, *193*, 109417. [[CrossRef](#)]
90. Pawlus, P. Simulation of stratified surface topographies. *Wear* **2008**, *264*, 457–463. [[CrossRef](#)]
91. Tang, J.; Chen, J.; Yang, D.; Li, L.; Zhao, J.; Guo, M. A new method of layered superposition reconstruction modeling on grinding-shot peening surfaces. *Surf. Topogr. Metrol. Prop.* **2020**, *10*, 045010. [[CrossRef](#)]
92. Pawlus, P.; Reizer, R.; Wiczorowski, M. A review of methods of random surface topography modeling. *Tribol. Int.* **2020**, *152*, 106530. [[CrossRef](#)]
93. Borodich, F.M.; Pepelyshev, A.; Savencu, O. Micro and nano scale statistical properties of rough surfaces of significance in their friction. In Proceedings of the 6th Vienna International Conference Nano-Technology—Viennano'15, Wiener Neustadt, Austria, 24–25 November 2015; Bartz, W.J., Franek, F., Eds.; The Austrian Tribology Society, (OETG): Wiener Neustadt, Austria, 2015; pp. 13–14.
94. Golyandina, N.; Zhigljavsky, A. *Singular Spectrum Analysis for Time Series*; Springer: Berlin/Heidelberg, Germany, 2020.

95. Borodich Suarez, S.; Pepelyshev, A. Study of impact of COVID-19 on industrial production indices using singular spectrum analysis. *Stat. Its Interface* **2023**, *16*, 181–188. [[CrossRef](#)]
96. Borodich Suarez, S.; Heravi, S.; Pepelyshev, A. Forecasting industrial production indices with a new singular spectrum analysis forecasting algorithm. *Stat. Its Interface* **2023**, *16*, 31–42. [[CrossRef](#)]
97. Borodich, F.M.; Pepelyshev, A. Synthesis of Engineering Surfaces using Representative Elementary Patterns of Roughness. 2024, *submitted*.
98. Polonsky, I.A.; Keer, L.M. A numerical method for solving rough contact problems based on the multi-level multi-summation and conjugate gradient techniques. *Wear* **1999**, *231*, 206–219. [[CrossRef](#)]
99. Polonsky, I.A.; Keer, L.M. Fast methods for solving rough contact problems: A comparative study. *J. Tribol.* **2000**, *122*, 36–41. [[CrossRef](#)]
100. Zhou, Q.; Jin, X.; Wang, Z.; Wang, J.; Keer, L.M.; Wang, Q. Numerical EIM with 3D FFT for the contact with a smooth or rough surface involving complicated and distributed inhomogeneities. *Tribol. Int.* **2016**, *93*, 91–103. [[CrossRef](#)]

Disclaimer/Publisher’s Note: The statements, opinions and data contained in all publications are solely those of the individual author(s) and contributor(s) and not of MDPI and/or the editor(s). MDPI and/or the editor(s) disclaim responsibility for any injury to people or property resulting from any ideas, methods, instructions or products referred to in the content.